Robust Link Adaptation In HSPA Evolved

DANIEL GÖKER

KTH Signals
Sensors and Systems

Master of Science Thesis
Stockholm, Sweden 2009

Robust Link Adaptation In HSPA Evolved

DANIEL GÖKER

KTH Signals
Sensors and Systems

Master of Science Thesis performed at
the Radio Communication Systems Group, KTH.
February 2009

Examiner: Professor S. Ben Slimane

KTH School of Information and Communications Technology (ICT)
Department of Communication Systems (CoS)

CoS/RCS 2009-03

Tryck: Universitetsservice AB

Abstract

This master thesis studies a robust link adaptation in HSDPA, with the use of dynamic Channel Quality Indicator (CQI) reports. Due to measurement error, quantization error and delay, the CQI estimated is not equal to the CQI experienced at reception and the error may result in a transport format not suitable for the channel conditions. The Block Error Rate (BLER) that follows does not achieve its target. The investigated algorithm adds an offset to the estimated CQI. The offset is a function of the UE mean speed and the target BLER, since the CQI error is varying with the speed. Applying this offset, the chosen target BLER should be reached on average. Simulations were carried out to compare robust link adaptation with the existing CQI adjustment, in terms of BLER stability and controllability. The results show that robust link adaptation fulfills both requirements, but cannot take interference variations into account – which may lead to incorrect BLER when the interference is changing. Robust link adaptation shows most gain over CQI adjustment at high speeds, and has same performance for all packet sizes, as opposed to CQI adjustment which needs large packets to gather error statistics. The offsets in a robust link adaptation system are partly based on an assumption on receiver type. Since the receiver types can vary in a network, CQI adjustment should be used in conjunction with robust offsets, to obtain both a degree of robustness and flexibility.

Acknowledgements

This master thesis project has been carried out on the department of Wireless Access Networks, Ericsson Research, Kista. I want to express my gratitude to Claes Tidestav who has been my advisor at Ericsson, and to Professor Ben Slimane, my examiner at KTH. They have given me great advice, supported and reviewed my work.

I would also like to thank my desktop neighbors, Mats Blomgren, Andreas Höglund and Henrik Nyberg, for several insightful discussions. It is essential to have people around you to exchange ideas with.

Finally I want to thank Ericsson for providing me this opportunity and chance to get experience in industrial research. The company has offered me great working resources as well as economical support.

Contents

List of Tables

List of Figures

List of Notations

R	Data Rate
$\bar{\cdot}$	Average Operator
$E[\cdot]$	Expected Value Operator
t	Time Instant t
$t+d$	Time Instant d Seconds After t
Γ	Stochastic SIR
γ	Outcome of Γ
X_{meas}	Stochastic Variable For Gaussian Measurement Error
μ_{meas}	Mean Value of Gaussian Measurement Error
σ_{meas}	Standard Deviation of Gaussian Measurement Error
X_{quant}	Stochastic Variable For Uniform Quantization Error
a_{quant}	Interval Limit For Uniform Quantization Error
T_c	Channel Coherence Time
B_D	Doppler Spread Spectrum
v	Speed
v_{mean}	UE Mean Speed
m	Nakagami Fading Parameter
α	Channel Gain
$\mathbf{\Gamma}(\cdot)$	Gamma Function
ρ	Correlation Coefficient
I_m	mth Order Modified Bessel Function of The First Kind
J_n	nth Order Bessel Function of The First Kind
L_P	Path Loss
L_S	Slow Fading Loss
P	Power
E_b	Bit Energy
N_0	Noise Power Spectral Density
λ	Arrival Intensity of Poisson Distribution

List of Abbreviations

3G	3rd Generation
3GPP	3rd Generation Partnership Project
ACK	Acknowledgment
BLEP	Block Error Probability
BLER	Block Error Rate
CC	Chase Combining
CDF	Cumulative Distribution Function
CPICH	Common Pilot Channel
CRC	Cyclic Redundancy Check
CQI	Channel Quality Indicator
DPCCH	Dedicated Physical Control Channel
DPDCH	Dedicated Physical Data Channel
F-DPCH	Fractional Dedicated Physical Channel
GIR	Gain to Interference Ratio
GRAKE	General RAKE
HARQ	Hybrid Automatic Repeat Request
HS-DPCCH	High Speed Dedicated Physical Control Channel
HS-DSCH	High Speed Downlink Shared Channel
HS-PDSCH	High Speed Physical Downlink Shared Channel
HS-SCCH	High Speed Shared Control Channel
HSDPA	High Speed Downlink Packet Access
HSPA	High Speed Packet Access
HSUPA	High Speed Uplink Packet Access
IP	Internet Protocol
IR	Incremental Redundancy
L1	Layer 1
L2	Layer 2
MAC-d	Medium Access Control Dedicated
MAC-hs	Medium Access Control High Speed
MCS	Modulation- and Coding Scheme
MIMO	Multiple Input Multiple Output
NACK	Negative Acknowledgement
PDCP	Packet Data Convergence Protocol
PDF	Probability Density Function

PDU	Packet Data Unit
PedA	Pedestrian A
PS	Packet Switched
QAM	Quadrature Amplitude Modulation
QPSK	Quadrature Phase Shift Keying
Ref	Reference case
RLC	Radio Link Control
RNC	Radio Network Controller
Rob	Robust case
SIR	Signal to Interference Ratio
TBSZ	Transport Block Size
TCP	Transmission Control Protocol
TP	Throughput
TTI	Transmission Time Interval
TU	Typical Urban
UE	User Equipment
UMTS	Universal Mobile Telecommunications System
UTRAN	UMTS Terrestrial Radio Access Network
WCDMA	Wideband Code Division Multiple Access

Chapter 1

Introduction

1.1 Background

3G evolution is driven by the demand for high data rates, low latency and capacity. The first release of the European system UMTS – 3GPP Release 99 – offered a peak data rate of 384 kbps. With the addition of High Speed Downlink Packet Access (HSDPA) in 3GPP Release 5, the downlink peak data rate was increased to 14 Mbps. Since there was also a demand for fast uplink, 3GPP Release 6 introduced Enhanced Uplink, also referred to as High Speed Uplink Packet Access (HSUPA), with peak rates of 5.8 Mbps. The combination of HSDPA and HSUPA is commonly referred to as HSPA. The latest available release has number 7, and is known as *HSPA Evolved*. It supports 42 Mbps in the downlink and 11 Mbps in the uplink.

The higher peak rates in HSPA Evolved have been achieved with higher order modulation, MIMO and an enhanced layer 2. Peak rates are rarely possible to reach, because of fading, interference and noise. Instead the highest possible data rate is selected, given the current conditions. This procedure is called link adaptation. To support the selection of a suitable rate, the channel quality indicator (CQI) indicates what the current conditions are at the receiver. The more accurate the link adaptation is, the better will the end-user and network performance be.

Because of complexity and resource limitations, the CQI and hence link adaptation cannot be completely accurate. This thesis work addresses what can be done to achieve good link adaptation performance, despite of the CQI inaccuracy. The outcome is a *robust link adaptation*.

1.2 Problem Definition

Link adaptation is essential in HSPA to maximize user and system throughput. How it works is explained in Section 2.5. This thesis will consider the downlink, i.e. HSDPA, as it is rate controlled. Rate control means that the base station controls the bit rate at which transmission to the user is done. The rate is adjusted by changing modulation order and/or channel-coding rate. A higher coding rate results in less overhead but reduces error-correcting capabilities. A higher modulation order will be capable of transmitting more bits per symbol,

but requires a higher received signal-to-interference ratio (SIR) for the symbols to be correctly received.

The standard does not dictate how base station should select rate, but it commonly uses the CQI reports from the users [1]. Each user measures its reception quality, maps the value to an m-bit number and transmits it to the base station. This is done at regular intervals, at most once every transmission time interval (TTI) which is 2 ms. The base station applies the data rate as soon as possible for the next transmission.

In the entire link adaptation procedure there are three obvious sources of inaccuracy. First, the measurement of reception quality can be assumed to be imperfect. Secondly, when quantizing the measured value, information is lost. The third source is because of the delay from the measurement until the transmitted data block is received. This delay includes transmission time, processing time, and the fact that the reporting interval may be long so the report may be old. During the delay both the fast fading and interference situation might change.

All these three sources of inaccuracy contribute to a data rate selection that isn't appropriate for the channel conditions. One doesn't want to choose a too low rate, not utilizing all the capacity. Also, a too high data rate will result in more bit errors. Both cases implies a lower throughput.

There is reason to believe that the link adaptation performance can be improved if the base station takes the CQI inaccuracy into account. The question to be answered is "Can we control the link adaptation accurately despite the imperfect CQI?". The motivation for a solution is to obtain higher system throughputs than in today's systems or, alternatively, to increase the reporting interval without degrading the system throughput.

1.3 Related Work

Since link adaptation is a key technology in order to make HSDPA work efficiently, a lot of research is being done optimizing it. To mitigate the result of inaccurate link adaptation, current implementations compensate after transmission by estimating the resulting block error rate and adjusting CQI accordingly [2]. Another approach has been prediction, to in some way predict what happens between two consecutive CQI reports, due to the fast fading. Some such techniques were tried in [3]. [4] investigates averaging over several CQI values (actually their corresponding SIR) to be less sensitive to rapid changes.

In some other works, focus is put on finding better alternatives to CQI reports. The approach in [5] eliminates CQI completely by implicitly estimating channel quality based on ACK/NACK from the UE. This showed to yield higher system throughput at high user speeds, but also a too high block error rate (BLER), compared to using explicit CQI reporting. Another scheme is to utilize the downlink power control. If the UE asks for high power, it means that its channel conditions are unfavorable. Combined with infrequent CQI reports, this scheme has showed to work quite well [1]. Also, [6] suggests that filtering off redundant CQI reports is a way of avoiding unnecessary uplink transmissions.

This thesis adds a novel method where the CQI reports are adjusted knowing the sources of inaccuracy. It is not an alternative to CQI reporting, but rather an improvement that makes it more confident.

1.4 Approach

The purpose of robust link adaptation is to be a safe method that selects the correct data rate no matter how inaccurate the CQI reports are. The approach is to adjust the CQI reports by some offset. The offsets depend on the measurement error, quantization error and UE speed. Using the offset CQI reports, the target block error probability (BLEP) should be reached on average.

A function will be implemented, which finds suitable offsets given the inaccuracy sources as input. Then the robust system will be compared to the present system in terms of BLEP stability and controllability. Tests will be conducted, that determines the target BLEP optimizing throughput. The goal is to let the offsets be found dynamically in the base station.

1.5 Outline

The report will be outlined as follows: Chapter 2 gives the necessary underlying theory, Chapter 3 describes the new algorithm in detail, Chapter 4 describes the simulator and what assumptions and implementations are made, Chapter 5 presents the simulation cases and the final results, and finishes off with comparisons and discussion of the results. Finally in Chapter 6, conclusions are drawn and possible/suitable future work is presented.

Chapter 2

Prerequisite HSPA Theory

The purpose of this chapter is to introduce important concepts of 3G networks to the reader, as well as making definitions that will be used later in the report. It will explain the technologies that are emphasized in the thesis: link adaptation, CQI and hybrid ARQ. The concepts and notions introduced here will be referred to in the following chapters.

2.1 HSPA And WCDMA In General

The radio access part of the Universal Mobile Telecommunications System (UMTS) is called UMTS Terrestrial Radio Access Network (UTRAN). The Frequency Division Duplex (FDD) part of UTRAN is called *Wideband Code Division Multiple Access* (WCDMA), and WCDMA is the technology used as air interface. The UTRAN is based on a hierarchical structure [7]. The base station is commonly referred to as *NodeB* and the devices utilizing the network are called User Equipment (UE). A number of NodeBs are controlled by a Radio Network Controller (RNC). The RNC contains most of the intelligence in the UTRAN, although more intelligence is being moved to the NodeB. The duties of the NodeB and RNC respectively will now be explained. Focus will be put on HSDPA, the downlink packet data service.

The radio access processing is structured into layers [8]. When IP packets arrive to the UTRAN, the processing starts at layer 2 (L2). L2 can be split into four sub-layers: PDCP, RLC, MAC-d and MAC-hs. The data flow through the layers is illustrated in Figure 2.1.

The IP packets arrive to the PDCP sub-layer which may compress the IP header. The resulting PDCP packet data unit (PDU) is passed to the RLC sub-layer, where it is divided into RLC PDUs of flexible size and an RLC header. The ability to adapt RLC PDU size is essential in HSPA Evolved, because if the PDUs are too small, they will limit peak data rates due to stalling (insufficient buffer window) [1]. The RLC PDUs are passed to the MAC-d sub-layer which optionally can add its own header. The PDCP, RLC and MAC-d sub-layers are all in the RNC, and they are of minor interest to this work.

More important is the L2 sub-layer called MAC-hs, residing in the NodeB. It contains the essential HSDPA functionality for scheduling, link adaptation and HARQ. The reason that it resides in the NodeB is that the functions depend

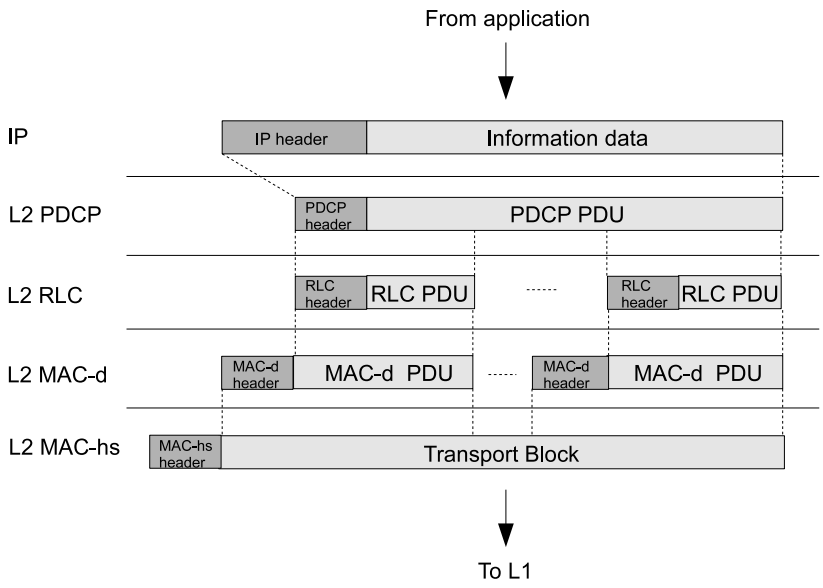

Figure 2.1: Data flow through UTRAN layers

on a low delay to the UE. The performance of scheduling, link adaptation and HARQ is directly related to how fast they can adapt to the current conditions. In the MAC-hs sub-layer, the MAC-d PDUs are segmented into smaller MAC PDUs to compensate for the flexibility in RLC PDU size previously mentioned. A number of MAC PDUs are assembled and a header is added. The result is a *transport block*, which is passed on to the physical layer (L1) – one every TTI. The NodeB also does all the physical layer processing: scrambling, coding, interleaving, modulation etc. The final result is symbols, ready for transmission.

For the transmission, WCDMA is the interface used. It uses channelization codes to make a physical separation between different channels. The coding makes the different channels orthogonal and spread in bandwidth. A channelization code spreads the original signal by a factor called *spreading factor*. One can achieve n orthogonal channels using spreading factor n. The higher the spreading factor is, the lower will the data rate be. Therefore there is a tradeoff between the number of channels and data rate of each channel.

2.2 Channel Structure In HSDPA

Channels carry data or control signalling in both uplink and downlink. A summary of the available channels is shown in Table 2.1.

Four of the channels are of great importance here, namely the HS channels and the CPICH. The *High Speed Downlink Shared Channel* (HS-DSCH) carries data to the UEs in the downlink. It is a transport channel that is shared among all UEs in a cell. The HS-DSCH can be configured to use between 1 and 15 *High Speed Physical Downlink Shared Channels* (HS-PDSCH) – each with a spreading factor of 16. The available HS-PDSCHs are dynamically shared to the UEs, both in time domain and code domain. For example, one UE can be

Table 2.1: Relevant HSDPA channels

Channel	Description	Type	Direction
HS-DSCH	User packet data	Shared	Downlink
HS-SCCH	Control signalling for HS-DSCH	Shared	Downlink
HS-DPCCH	Control signalling for HS-DSCH	Dedicated	Uplink
CPICH	Reference signalling for channel estimation	Shared	Downlink
F-DPCH	For circuit switched data and power control commands	Dedicated	Downlink
DPDCH	User data	Dedicated	Uplink
DPCCH	Control signalling for DPDCH	Dedicated	Uplink

given 5 codes and another 10 codes at one time instant. The next instant the distribution may be different.

The HS-DSCH has two physical control channels associated with it. In the downlink there is the *High Speed Shared Control Channel* (HS-SCCH) which carries signalling from the NodeB to the UEs. In the uplink there is the *High Speed Dedicated Physical Control Channel* which is unique for each UE.

The *Common Pilot Channel* (CPICH) is used for transmission of a known sequence. The UEs use this to estimate their channel conditions. This is essential and will come in handy later on, for the CQI.

NodeB resources in the downlink are limited by the amount of available power and number of codes. The dedicated channels are therefore power controlled to use as little power as needed. The power that is left is used for HS-PDSCH. The HS-PDSCH potentially gets all the remaining power to achieve as high data rate as possible.

2.3 Channel Dependent Scheduling

Scheduling controls the assignment of resources to the users. It is done in the NodeB and MAC-hs layer. The HS-DSCH is scheduled to one or more users on a per TTI basis. The scheduler can take into account both traffic conditions and channel conditions. For example, only users with data to transmit or receive need to be scheduled.

There are different strategies for how to schedule users based on their channel conditions. The simplest approach is called *Round-robin*. In Round-robin, the channel conditions are simply ignored. Users with data to transmit are scheduled in order and everyone gets the same time. This strategy provides maximum time fairness to the users, but cannot guarantee any quality of service. Users may be scheduled even if their channel conditions unables them to receive properly. The result is unused capacity.

The opposite extreme scheduling strategy is called *Max-C/I*. Here instead the user with the best instantaneous channel conditions is scheduled. This means for example that users close to the cell border are unlikely to be scheduled at all. Thus, Max-C/I is least fair to the users, but maximizes the system throughput in case all users have data to transmit.

In between Round-robin and Max-C/I lies the *Proportional-fair* scheduler. It

schedules the user that has the best channel conditions compared to its average channel quality. This way the scheduler maximizes system throughput while still being fair. Mathematically, the scheduled user n can be found as

$$n = \arg\max_i \frac{R_i}{\overline{R_i}} \tag{2.1}$$

where R_i is the instantaneous achievable data rate for user i.

Both the Proportional-fair and Max-C/I schedulers need information about the channel quality seen by the users as input. CQI reports serve as means for this purpose.

2.4 Hybrid ARQ

Automatic Repeat reQuest (ARQ) adds the ability to retransmit erroneous blocks. Data transmission often requires very low bit error rates, and HARQ is powerful for this purpose.

All transport blocks comes with a CRC code, and after decoding, the block is checked for errors. The result is indicated by a 1-bit (0 or 1) number and transmitted to the NodeB over the HS-DPCCH channel. If the block is error-free, ACK (1) is sent. If an error is detected instead, a NACK (0) is sent. In case of a NACK, the NodeB retransmits the same block again. The process is repeated until ACK is received, or until the maximum number of retransmissions has been reached.

In Hybrid ARQ, when a block contains errors it is not discarded, but instead buffered. The information from all of the received versions of the same block is then combined. This increases the probability of successful decoding. Combining can either be performed using soft information or hard bits. There are two types of soft combining commonly used in HSDPA – *Incremental Redundancy* (IR) and *Chase combining*. In IR, each version of the block contains different redundancy versions that can be put together to get even more redundancy. This results in a coding gain, since the code rate becomes lower for each retransmission. Using Chase combining, the same code is used for every retransmission. No coding gain is therefore achieved, but for each added soft block, a 3 dB diversity gain in E_b/N_0 is seen.

2.5 Link Adaptation

Link adaptation is about rate control, and it is closely related to channel dependent scheduling. Also residing in the MAC-hs layer, the link adaptation adjusts the data rate per TTI to match the instantaneous channel conditions. Channel conditions in this case translates to *Signal-to-Interference Ratio* (SIR). SIR is here defined to include both interference and thermal noise. The data rate is adjusted by changing modulation and/or coding rate. A set of modulation and code is called a *Modulation- and Coding Scheme* (MCS). The higher the modulation order and code rate is, the more bits can be squeezed into the unit that is transmitted in one TTI – the *transport block*.

The NodeB chooses MCS for the scheduled user (or users). This is usually done based on CQI reports, but it may do the selection by any other means – no

standard exists. The MCS must be chosen with care in order to keep the block error rate (BLER) low. For a certain SIR, if one chooses too high modulation order or too high code rate, the BLER will be too high. If vice versa, one chooses too low modulation order or too low code rate, the link will not be fully utilized. For a given MCS, the characteristics of block error probability (BLEP) versus SIR looks like in Figure 2.2. Using this MCS for transmission, the BLEP would have been 10% if the received SIR was about 4.6 dB.

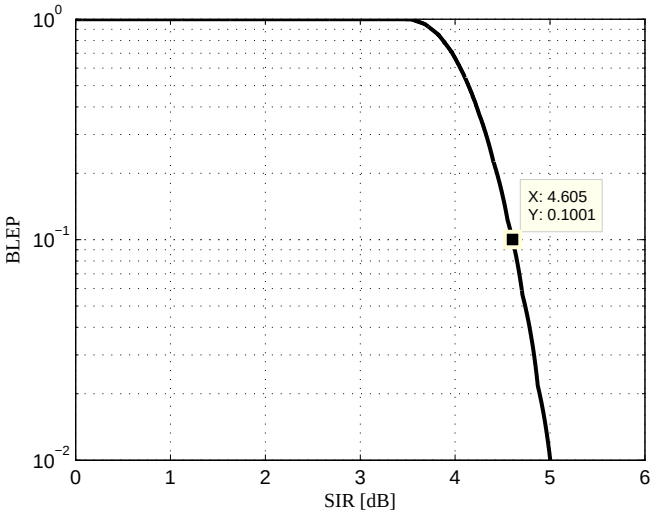

Figure 2.2: Characteristics of block error probability (BLEP) versus SIR, for a certain MCS

SIR in the figure refers to the SIR at which the transport block is received. BLEP refers to the probability that the transport block contains any error after demodulation and decoding. Errors occur when a received symbol is misinterpreted as another one, because of too low SIR. But depending on the code rate, a number of errors can be corrected. HSPA usually tries to operate at a BLEP of 10%, i.e. $\text{BLEP}_{\text{target}} = 10\%$. This means that the link adaptation will choose the MCS that results in 10% BLEP for the current SIR.

Say there are a set of N MCSs, $\{\text{MCS}_1, \text{MCS}_2, ..., \text{MCS}_N\}$. MCS_n corresponds to a data rate of R_n. The SIR range is split into $N + 1$ intervals, and MCS_n will be used of the SIR falls into the interval $[\text{SIR}_n, \text{SIR}_{n+1})$. The interval is chosen such that $\text{BLEP} = \text{BLEP}_{\text{target}}$. $\text{SIR} = \text{SIR}_n$ is denoted as the *SIR threshold*.

The selected MCS together with the number of channelization codes to transmit on, supports a certain *Transport Block Size* (TBSZ). This leaves 254 different TBSZs in HSDPA if only considering QPSK and 16QAM as modulation schemes [1]. 63 of these TBSZs can be used for each number of channelization codes. The TBSZ is adapted by assembling a number of MAC PDUs. To summarize, the TBSZ (and hence the data rate) is based both on the supported MCS at the given target BLEP, the number of codes scheduled to the UE, and the UE capabilities. The modulation order and number of codes shall never exceed the supported maximum in the UE.

An MCS, TBSZ and channelization code set together are called a *transport format*. It contains all the information needed to perform a transmission from the NodeB to the UE. First, the transport format has to be signalled to the UE, so that it knows how to use the data. This is done on the HS-SCCH channel (see Section 2.2). The transmitted information also contains a UE ID which identifies the UE that the transmission is intended for.

2.6 CQI

As mentioned before, both scheduling and link adaptation are done per TTI and based on the UE's channel conditions. For the assessment of downlink channel quality, the *Channel Quality Indicator* (CQI) is essential. CQI is input to both link adaptation and scheduler. The CQI reports going into the scheduler are not touched in this work. They are handled just as before and not subject to any robustness.

2.6.1 Measurement of CQI

Every UE (whether it has data to transmit or not) in a system continously measures its received SIR on the CPICH channel. At regular intervals, the measurement is averaged over an entire TTI (2 ms) and the value is saved. Denote the measured value by $\mathrm{SIR}_{\mathrm{CPICH}}$. The expected received SIR at time t on the HS-DSCH channel is then estimated as

$$\mathrm{SIR}_{\mathrm{t}} = \mathrm{SIR}_{\mathrm{CPICH}} + \phi \ \ [\mathrm{dB}] \tag{2.2}$$

where ϕ is the difference in transmission power between HS-DSCH and CPICH, signalled by the NodeB.

$\mathrm{SIR}_{\mathrm{t}}$ is then quantized and truncated into a discrete CQI value between 0 and 30, represented by 5 bits [1]. Finally, the 5-bit CQI value is transmitted to the NodeB over the HS-DPCCH channel (see Section 2.2).

2.6.2 CQI Processing in NodeB

From the CQI reports, the NodeB have to assess each UE's channel quality. It is known that the reported CQI is not always true, and therefore the current implementation lets the reports undergo *CQI adjustment*. The adjustment algorithm gradually modifies the CQI based on ACKs and NACKs, according to [2]. The NodeB uses the HARQ feedback to adjust the CQI up or down in steps of 1. The expression for adjusted CQI is

$$\mathrm{CQI}_{\mathrm{adj}} = \mathrm{CQI} + \Delta\mathrm{CQI} \tag{2.3}$$

where ΔCQI is adjusted based on the ACK and NACK flags. A large amount of statistics is required to form a confident estimate of the BLER at the UE. Unfortunately smaller transmissions will not have time to gather statistics fast enough. Therefore the adjustment algorithm has been divided into two parts: short-term and long-term adjustment.

[1] In a MIMO system each stream is represented by a 4 bit CQI value

Short-term CQI adjustment

The short-term CQI adjustment is meant to adjust CQI reports that deviate from the actual quality from the start. This is important for example when the user packet size is small. The algorithm is active the first N transmissions of a UE's life time. It performs the following adjustments:

$$\text{If 10 consecutive ACKs are received, } \Delta\text{CQI} = \Delta\text{CQI} + 1 \tag{2.4}$$

$$\text{If 2 consecutive NACKs are received, } \Delta\text{CQI} = \Delta\text{CQI} - 1 \tag{2.5}$$

Long-term CQI adjustment

The long-term CQI adjustment starts after N transmitted blocks of a user packet. The value of ΔCQI at the end of the short-term adjustment is kept when proceeding into long-term adjustment. In the long-term adjustment instead, the NodeB forms an estimate of the BLER based on M ACK/NACK flags. Then it performs the following adjustments:

$$\text{If estimated BLER is less than a lower threshold, } \Delta\text{CQI} = \Delta\text{CQI} + 1 \tag{2.6}$$

$$\text{If estimated BLER is larger than an upper threshold, } \Delta\text{CQI} = \Delta\text{CQI} - 1 \tag{2.7}$$

If CQI = 0, the report is excepted from CQI adjustment. CQI = 0 always means that no transmission is carried out.

Estimating channel quality experienced by the UE

The process of mapping SIR_t to CQI done by the UE, can at this point be reversed. CQI is converted back to a continuous number, but information has been lost:

$$\text{SIR}_{\text{t,estimated}} = \text{SIR}_{\text{CPICH}} + \phi \ \ [\text{dB}]. \tag{2.8}$$

Then, by removing ϕ and the CPICH power, only the Gain-to-Interference Ratio (GIR) is left:

$$\text{GIR}_{\text{t,estimated}} = \text{SIR}_{\text{CPICH}} + \phi - \text{P}_{\text{CPICH}} - \phi = \text{GIR}_{\text{CPICH}} \ \ [\text{dB}] \tag{2.9}$$

The NodeB knows the power it can allocate for HS-DSCH transmission to the UE. By adding that power to the GIR, the SIR that is achievable on the HS-DSCH is found. An offset called *channel quality offset* is also removed. This offset is a safety backoff, so that the SIR used for TBSZ selection is initially underestimated. The final expression for the SIR that the NodeB thinks the UE will achieve, becomes

$$\text{SIR}_{\text{achievable}} = \text{GIR}_{\text{t,estimated}} + \text{P}_{\text{HS-PDSCH}} - \text{ChQualOffset} \ \ [\text{dB}]. \tag{2.10}$$

A common value for the channel quality offset is ChQualOffset = 2 dB. It has been determined from the typical working point for CQI adjustment. When aiming for 10% BLEP, experiences show that ΔCQI converges to -2. Hence it is good to start at that point.

2.6.3 CQI Application And Delay Analysis

$\text{SIR}_{\text{achievable}}$ is the input to the link adaptation, which uses it to choose transport format. Transmission is carried out and the block is received at time $t + d$ and with SIR_{t+d}.

The delay d from the time of measurement until block reception comprises different delay sources, as depicted in Figure 2.3. A TTI can be divided into three slots, 2/3 ms each. Transmission of the CQI report starts one slot after the measurement, mainly because of processing delay [1]. The report is received in the NodeB two slots later. Then it takes the NodeB about 2.5 slots to make a decision about scheduling and transport format. The decision is signalled and two slots later data transmission starts. The total delay adds up to about 7.5 slots, or 5 ms.

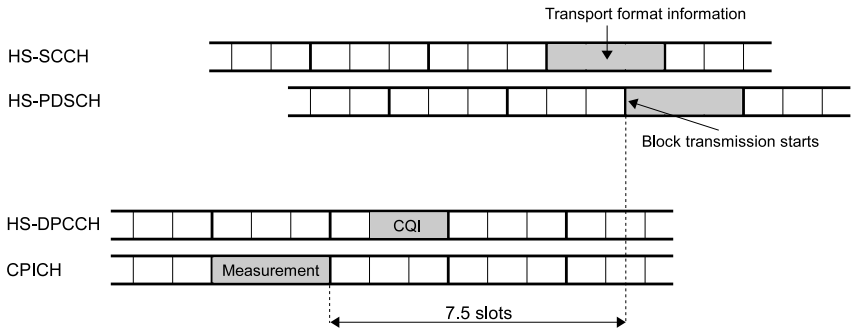

Figure 2.3: CQI delay illustration

In the above delay analysis, an assumption was made that the CQI is reported every TTI. The reporting interval is configurable between 1-80 TTIs [1]. Obviously, the larger interval, the larger will the delay d be. But d will also be varying – when the CQI report is fresh, d is small, but the CQI report will get older for each TTI until a new report arrives. The variation is not handled in this work.

Chapter 3

Robust Link Adaptation

3.1 Idea Description

In all link adaptation, it is desired that the transmission data rate is adapted to the exact condition at the time of reception. No system does this perfectly, and this is where improvements are needed. Denote by Γ_t the received HS-DSCH SIR at time t (previously denoted as $\mathrm{SIR_t}$), and by Γ_{t+d} the HS-DSCH SIR at the time the block is received (previously denoted as $\mathrm{SIR_{t+d}}$). The ideal situation would be that $\Gamma_{t+d} = \Gamma_t$, in which case BLEP = BLEP$_t arget$. There are three dominant reasons that this does not hold in reality.

CQI measurement error

Each UE measures its received SIR on the CPICH channel. Because of complexity limitations and natural inaccuracies, the measurement is not entirely precise. To model this, a random measurement error will be added, described by the stochastic variable X_{meas}. X_{meas} can be modelled by a log-normal distribution with mean μ_{meas} and standard deviation σ_{meas},

$$X_{meas} \in N\left(\mu_{meas},\ \sigma_{meas}\right) \quad [\mathrm{dB}] \tag{3.1}$$

Quantization and truncation error

At the mapping from SIR to CQI, SIR is quantized and truncated. This adds a random error X_{quant} which is uniformly distributed in the symmetric interval $[-a_{quant},\ a_{quant}]$. The truncation may introduce larger errors, but this will be avoided in the simulations.

Delay error

Denote by d the interval from the time of SIR estimation until the block is received. During this time, the link quality will change due to fast fading and interference variations. The interference is always there as long as there are other active users in the system, and its impact on the SIR cannot be predicted in a good way. The fast fading is caused by time dispersion of the different

multipath components, and random frequency modulation of the different components caused by Doppler shift. In analysis, a flat fading channel (no time dispersion) is often used. Still, at high speeds, the Doppler shift is substantial. The *coherence time* T_c is a measure of the time duration over which the channel impulse response is constant. It is approximately inversely proportional to the Doppler spread B_D caused by the movement,

$$T_c = \frac{1}{B_D} \tag{3.2}$$

and the Doppler spread depends on the carrier frequency, the UE speed and the speed of light,

$$B_D = \frac{f_c v}{c} \tag{3.3}$$

The channel coherence time quickly gets small as the speed increases, as showed in Figure 3.1. If the channel coherence time is smaller than the link adaptation delay, that is, if $T_c < d$, then Γ_t can not reflect the SIR that will be experienced d seconds later.

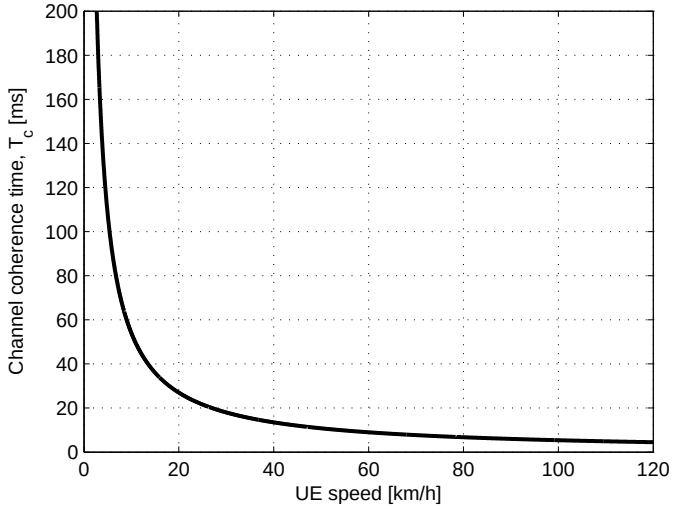

Figure 3.1: Channel coherence time versus UE speed

A wide range of fast fading channels can be modelled by the *Nakagami-m* distribution [10]. The m parameter can be used to fit the distribution to different environments. Rayleigh distribution is the special case when $m = 1$. The PDF of the channel gain α in a Nakagami-m fading channel is given by

$$p_\alpha(\alpha) = 2\left(\frac{m}{\Omega}\right)^m \frac{\alpha^{2m-1}}{\mathbf{\Gamma}(m)} \exp\left(-m\frac{\alpha^2}{\Omega}\right), \quad \alpha \geq 0 \tag{3.4}$$

where $\mathbf{\Gamma}(.)$ is the gamma function and $\Omega = E(\alpha^2)$ is the average fading power. The PDF of the received SIR is then gamma distributed [11],

$$p_{\Gamma}(\gamma) = \left(\frac{m}{\bar{\gamma}}\right)^{m} \frac{\gamma^{m-1}}{\mathbf{\Gamma}(m)} \exp\left(-m\frac{\gamma}{\bar{\gamma}}\right), \quad \gamma \geq 0 \tag{3.5}$$

where $\bar{\gamma}$ is the average received SIR. Given a SIR at time t, Γ_t, the conditional PDF of the SIR at time $t+d$ if only affected by the Nakagami-m fading (nmf), Γ_{nmf}, can be found as in [11],

$$\begin{aligned} p_{\Gamma_{nmf}|\Gamma_t}(\gamma_{nmf} \mid \gamma_t) &= \frac{m}{(1-\rho)\bar{\gamma}_{nmf}} \left(\frac{\gamma_{nmf}}{\rho\gamma_t}\right)^{(m-1)/2} I_{m-1}\left(\frac{2m\sqrt{\rho\gamma_t\gamma_{nmf}}}{(1-\rho)\bar{\gamma}_{nmf}}\right) \cdot \\ &\cdot \exp\left(-\frac{m(\rho\gamma_t + \gamma_{nmf})}{(1-\rho)\bar{\gamma}_{nmf}}\right) \end{aligned} \tag{3.6}$$

where $I_{m-1}(.)$ is the (m-1)th order modified Bessel function of the first kind. ρ is the correlation coefficient of Γ_{nmf} and Γ_t. When ρ is small (close to 0), Γ_{nmf} is uncorrelated with Γ_t. A large ρ (close to 1) on the other hand means that $\Gamma_{nmf} = \Gamma_t$. ρ depends on the Doppler spread and delay d as

$$\rho = J_0^2(2\pi B_D d) \tag{3.7}$$

where J_0 is the zero order Bessel function of the first kind. The PDF of Γ_{nmf} in linear scale and for different values of m is shown in Figure 3.2 and 3.3 for 3 and 50 km/h respectively.

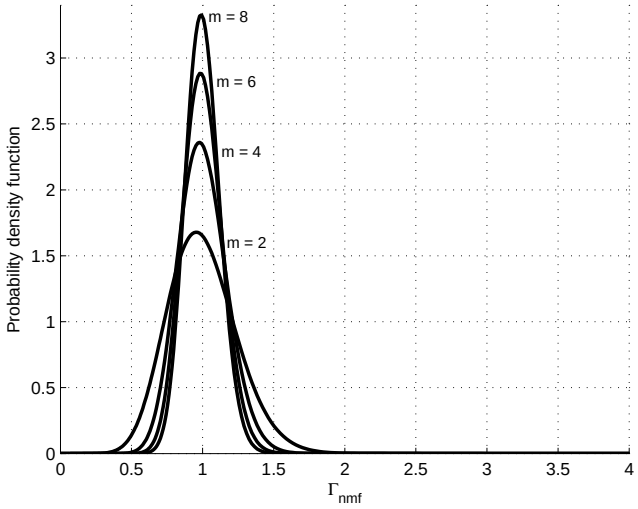

Figure 3.2: PDF of Γ_{nmf} in linear scale, given that $\Gamma_t = 1$. The UE speed is 3 km/h and $d = 10$ ms

Total CQI error

The sources of error are independent of each other. If we put together the measurement error, quantization error and delay error, we can get an expression

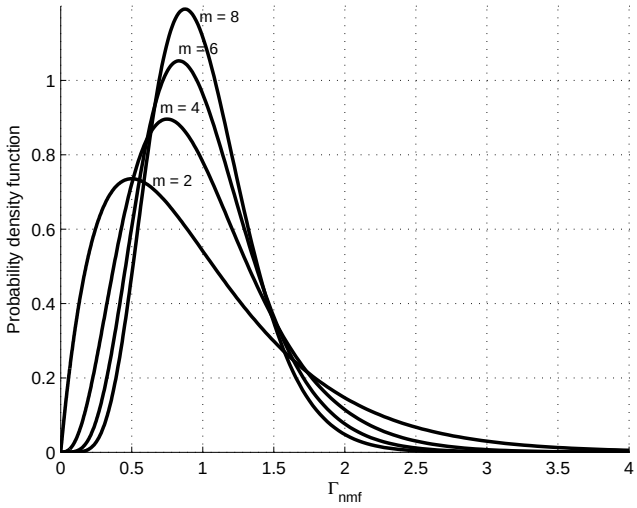

Figure 3.3: PDF of Γ_{nmf} in linear scale, given that $\Gamma_t = 1$. The UE speed is 50 km/h and $d = 10$ ms

for the received SIR at time $t + d$, Γ_{t+d}. The contribution from interference is also there, but is unknown.

$$\Gamma_{t+d,\,dB} = \Gamma_{nmf,\,dB} + X_{meas} + X_{quant} + \text{Interference} \tag{3.8}$$

Resulting problem

As described in Section 2.5, the BLEP will depend on Γ_{t+d} and the MCS used. Take as an example a target BLEP of $\text{BLEP}_{\text{target}} = 10\%$. For a certain MCS n, the target BLEP will only be achieved at one specific SIR. But since Γ_{t+d} is a stochastic variable, BLEP will also be stochastic. This is illustrated in Figure 3.4. The curve is steep at the working point. Hence a small change in Γ_{t+d} will result in a large change in BLEP.

The mapping from Γ_{t+d} to BLEP is a non-linear function [12]. As a result of this, we have that

$$E\left[\Gamma_{t+d}\right] = \Gamma_t \Longrightarrow E\left[\text{BLEP}\right] = \text{BLEP}_{target} \tag{3.9}$$

where E[.] is the expected value. In words, it means that even if Γ_{t+d} is unbiased, BLEP will still be biased.

Because of the fading, scheduling policy and other influences, it is not obvious that Γ_{t+d} will be unbiased. Also, when Γ_t is large, it is more probable that the channel quality will go down than up during the delay [12] – and vice versa.

The idea

Split Γ_{t+d} into two parts,

$$\Gamma_{t+d} = \Gamma_t + \Gamma_e \tag{3.10}$$

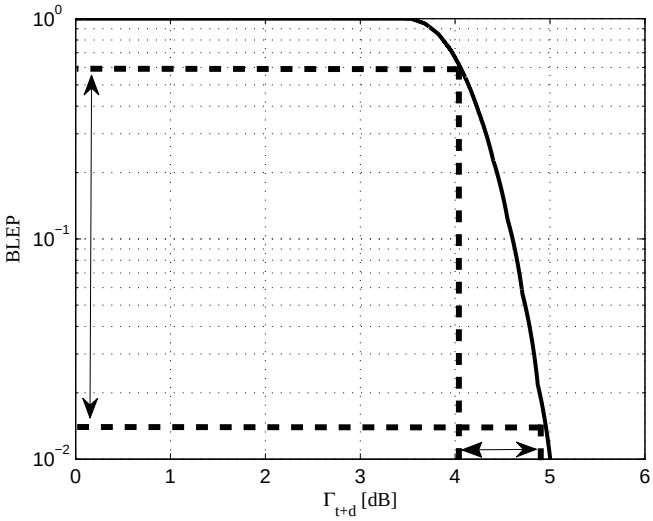

Figure 3.4: Variation in Γ_{t+d} resulting in variating BLEP

where Γ_e is the *SIR error distribution*, comprising all error sources. Present systems assume that $\Gamma_e = 0$, i.e. $\Gamma_{t+d} = \Gamma_t$. Under this assumption, MCS is chosen based on the Γ_{t+d} that results in BLEP = BLEP$_{target}$, see Figure 3.5. It is known that the assumption $\Gamma_e = 0$ is incorrect and that is the reason why CQI adjustment has been needed.

A robust link adaptation assumes

$$\Gamma_e \neq 0, \tag{3.11}$$

$$E[\Gamma_e] = 0, \tag{3.12}$$

$$V[\Gamma_e] = \sigma_e^2. \tag{3.13}$$

In the nominal case, when $\sigma_e > 0$, we have that $E[\text{BLEP}] \neq \text{BLEP}_{target}$. In a robust link adaptation, BLEP should be correct on average despite the Γ_{t+d} distribution. A new way of choosing MCS therefore has to be introduced. It should map $E[\Gamma_{t+d}]$ to $E[\text{BLEP}]$, knowing the value of σ_e. An example of this mapping with a certain σ_e is depicted in Figure 3.6. The new mapping has higher SIR threshold than the old mapping for a given MCS. Another way to achieve the same effect is to use a channel quality offset (just as in CQI adjustment) to lower the SIR that the MCS selection is based on.

It would be preferable to estimate σ_e directly in the NodeB, although this requires knowledge of Γ_{t+d}. Instead, σ_e has to be assessed knowing the error sources. For a given UE, some sources such as σ_{meas}, a_{quant} and d, are static. Interference can vary but not in a predictable way. Most importantly, the UE speed can vary and affect σ_e. The channel quality offset (ChQualOffset) therefore has to vary with speed. ChQualOffset can be based on the average UE speed v_{mean} to achieve good average system performance, or derived for each UE which is more complicated. The latter method is not considered in the simulations, but should be used in real systems.

In case Assumption 3.12 would not be true for some reason, the bias must

be removed so that $E[\Gamma_{t+d}] = \Gamma_t$. This is easily performed as soon as the error distribution is estimated or calculated.

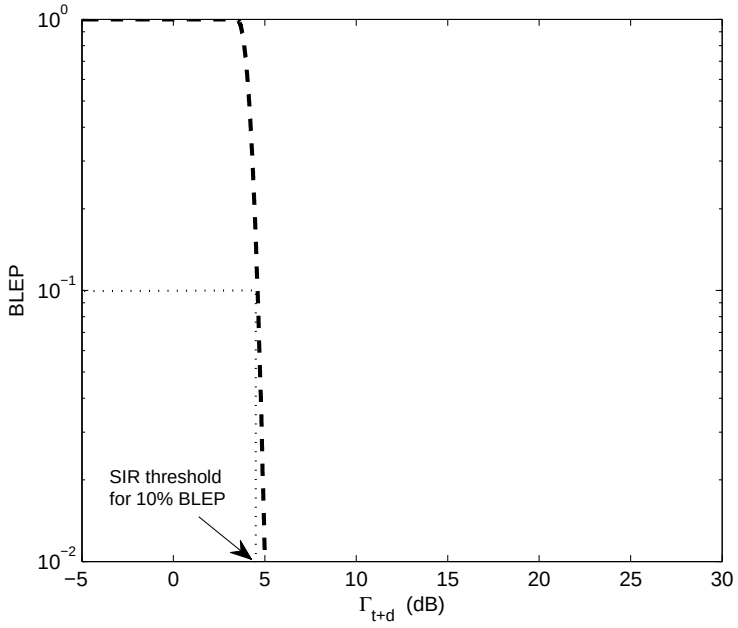

Figure 3.5: SIR to BLEP mapping in present systems, for a certain MCS n

3.2 Algorithm Details

In a real system or even in a simulator, the Γ_{t+d} distribution comprises many factors that cannot be easily modelled, and is not a simple analytic expression. The channel is not flat, interference exists, most receivers can mitigate some multipath fading etc. Therefore it is not possible to find an analytical model for ChQualOffset as a function of v_{mean}. Instead an empirical distribution will be used as a basis for the algorithm. The algorithm works in the following steps:

1. At different v_{mean}, observe a large number of values from Γ_e to be able to approximate its distribution.
2. Assuming that $E[\Gamma_e] = 0$, vary Γ_t and study the resulting $E[BLEP]$ at MCS n.
3. When $E[BLEP] = BLEP_{target}$, choose that Γ_t as threshold for MCS n.
4. The channel quality offset is calculated as

$$\text{ChQualOffset} = \text{New threshold} - \text{Old threshold}, \tag{3.14}$$

which is illustrated in Figure 3.7.

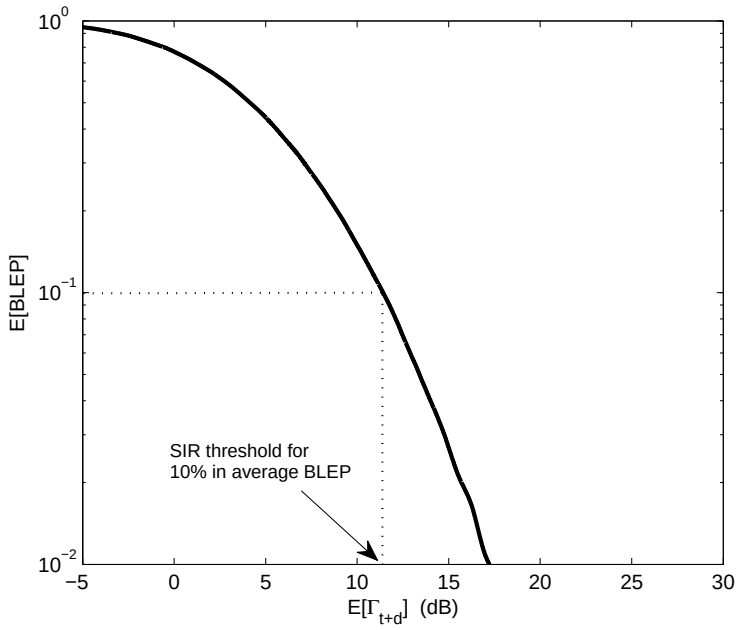

Figure 3.6: Mean SIR to mean BLEP mapping in a robust system, for MCS n and a certain Γ_e

5. Remove the bias $E[\Gamma_e]$ to make sure that SIR is estimated correctly on average:

$$\text{ChQualOffset} := \text{ChQualOffset} - E[\Gamma_e] \tag{3.15}$$

6. Repeat step 2–5 for all MCSs.

7. Repeat step 1–6 for all v_{mean} that are of interest. To obtain offsets for *any* v_{mean}, interpolation can be done.

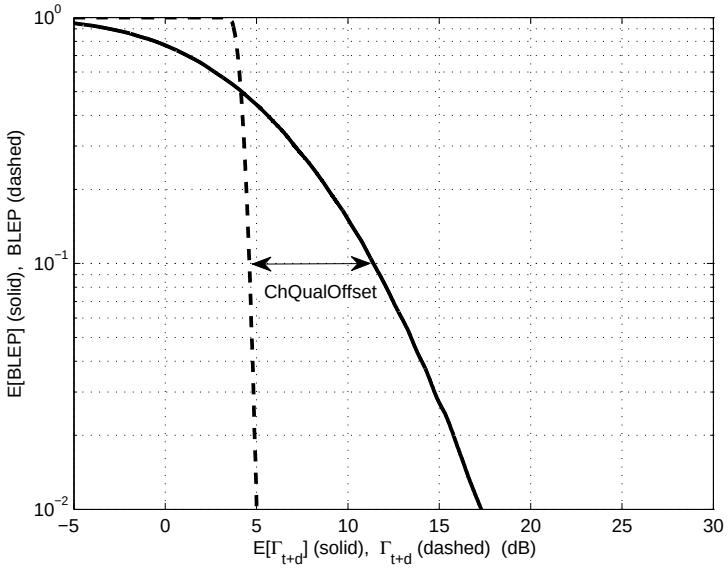

Figure 3.7: Determining ChQualOffset at 10% in target BLEP, for MCS n and a certain Γ_e

Chapter 4

Simulation Models

This chapter will introduce the system simulator used to implement the algorithms and conduct tests. It will explain the implementations done and what models and assumptions have been used.

4.1 General About The Simulator

A Matlab based simulator developed by Ericsson Research is used. It implements simplified models of most UTRAN functionalities and features HSPA and its evolution. Models in the simulator include network layout models, propagation models, user mobility, traffic generation and radio functionality. Instead of dividing the network into nodes – such as UE, NodeB and RNC – the simulator divides it into functions, such as SIR estimation, scheduling, handover etc. This way it is easy to evaluate each functionality separately.

4.2 Models And Assumptions

This section presents the models and assumptions adopted in this study. A table summary of all parameters can be found in Appendix B, Tables B-B.

4.2.1 System Model

The network consists of three sites. Each site contains three base stations, each of them covering 120°. This leaves a total of 9 hexagonal cells, as illustrated in Figure 4.1. To make sure that a user experiences the same inter cell interference in the middle of the system as on the border, a technique called *wrap-around* is used. Wrap-around connects the edges with each other so that a user moving outside the border appears on the other side of the system. It can be seen as copies of the original network, surrounding it. The site-to-site distance is set to 1500 m, which results in a cell radius of 500 m.

A 2D antenna model is adopted, with a gain pattern as in Figure 4.2. The gain varies in azimuth, but not in elevation. The height of the antenna is 30 m.

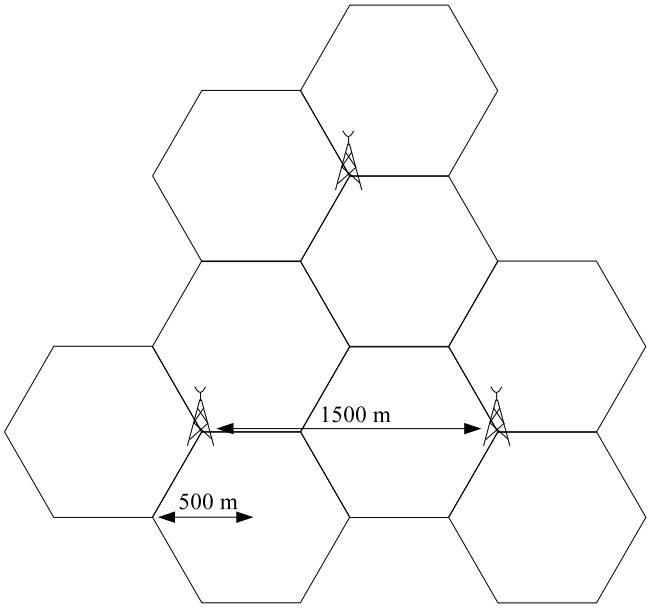

Figure 4.1: Simulated network illustrated without wrap-around

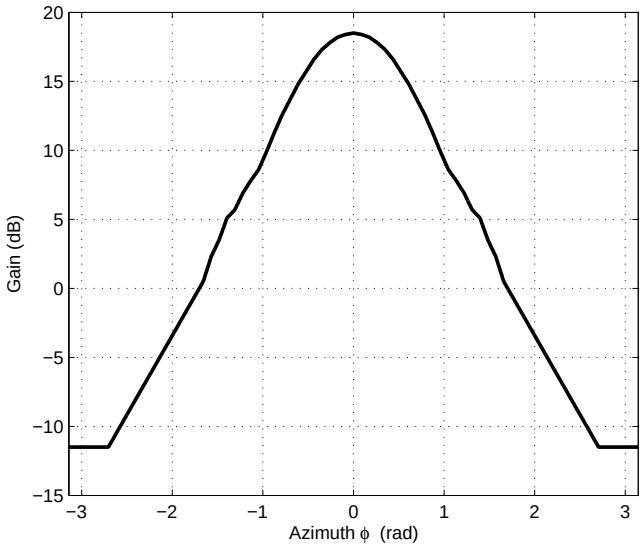

Figure 4.2: Antenna gain pattern (constant in elevation, θ)

4.2.2 Channel Model

The path loss between NodeB and UE can be divided into three main components: distance-dependent path loss, shadow fading and fast fading.

Distance Dependent Path Loss

The signal attenuates proportional to the distance d between NodeB and UE. The empirical Okumura-Hata model describes the attenuation [13]:

$$L_P(d) = C + \beta \log_{10}(d) \quad [dB] \tag{4.1}$$

where the parameters C and β depend on e.g. the base station height, carrier frequency and area type. For the simulations an urban area type is used, $C = -29.0125$ and $\beta = -3.5225$.

Shadow Fading

Slow fading occurs when the channel changes over several symbols. A common cause is shadowing due to large obstacles. In the simulator, shadow fading is modelled by a log-normal distribution [13]:

$$L_S \in N(0,\, 8) \quad [dB] \tag{4.2}$$

The decorrelation distance is set to 100 m. The slow fading is implemented by precomputed fading maps to increase simulation speed and ensure that the same position always results in the same fading.

Fast Fading

Fast fading occurs when the channel changes during one symbol interval. This is due to multipath propagation of the signal. The multipath fading is modelled by precomputed fading maps to increase simulation speed and ensure that the same position always results in the same fading. The herein chosen fading map is *ITU Pedestrian A* (PedA).

To mitigate the effect of multipath fading, the UEs employ GRAKE receivers of type GRAKE2 – with two antennas. The receiver is used together with an equalizing filter. The GRAKE receiver consists of several receivers (called fingers) receiving the different paths independently. It then combines them to achieve diversity.

4.2.3 Traffic Model

User Arrival and Load

The network can be seen as a queueing system. The arrivals are either bits or users. The network's capacity is limited both in bit rate and user capacity. The number of bits arriving to the system per second forms the *offered load* [bits/s/cell]. For a certain *mean packet size*, the user arrival intensity λ is given by

$$\lambda = \frac{\text{offered load}}{\text{mean packet size}} \quad [\text{users}/s/\text{cell}]. \tag{4.3}$$

New users are generated according to a Poisson process, and placed uniformly in the entire system.

The initial number of users depends on the offered load and an estimated bit rate. The bit rate is often underestimated, but all simulations start with

at least one user/cell and builds up to a steady number. Since the focus is on HSDPA, users are only downloading. A TCP model is not simulated.

Traffic Type

Only packet switched (PS) data is considered. Users are downloading fixed size packets over the HS-DSCH channel. They stay in the system until the download is complete. In a real system, UEs have different capabilities based on their complexity and what standards they support. Therefore they are categorized into 20 categories [14]. In the simulations, only category 8 is considered. It supports the following:

- Maximum number of HS-DSCH codes is 10
- Maximum transport block size is 14411 bits/TTI
- Supported modulation schemes are QPSK and 16QAM

64QAM modulation and Multiple-Input-Multiple-Output (MIMO) antennas are not simulated.

4.2.4 Radio Resource Management

Scheduling

Round Robin serves as scheduling policy for all simulations. It does not use CQI as input – users are scheduled merely in turn. Proportional Fair, for example, would schedule users that overestimates their SIR, more often. That would affect the SIR error distribution and hence the results.

Link Adaptation and CQI

The link adaptation uses $SIR_{achievable}$, calculated as in Section 2.6.2, to map into a suitable MCS. The mapping is done based on table lookup in a table of 601 MCSs. For UE category 8, only the first 285 MCSs can be used. MCS #1 is chosen based on special conditions, and is therefore disabled in the simulations.

The SIR measurement error is log-normally distributed with mean 0 dB and standard deviation $\sigma_{meas} = 1$ dB. No measurement bias is introduced. The difference in transmission power between HS-DSCH and CPICH, ϕ (defined in Section 2.6.1), is set to 7. The quantization and truncation which then takes place, gives a discrete CQI value between 0 and 30. The error lies in the interval [-0.5, 0.5]. The software simulates the delay from the SIR measurement is done until MCS is selected, in steps of 1 TTI. It is set to $d = 2\,\text{TTI} = 4\,\text{ms}$. The CQI reporting interval is set to $cqirepinterv = 4\,\text{TTI} = 8\,\text{ms}$. The oldest CQI reports used will hence be $d + cqirepinterv = 12$ ms old. CQI is assumed to be fed back without any error.

The long term CQI adjustment does averaging over 50 ACK/NACK reports, $M = 50$. The BLER estimate threshold for increasing CQI is $nackPlus = \text{BLEP}_{\text{target}} - 0.02$, and for decreasing CQI, $nackMinus = \text{BLEP}_{\text{target}} + 0.02$.

Hybrid ARQ

Hybrid ARQ adds the ability to retransmit erroneous transport blocks. If an error is detected after decoding, NACK is fed back to the NodeB. Otherwise ACK is fed back. The feedback is assumed error-free. In case of NACK, the same block is transmitted again and combined with previously received copies in the receiver, using Chase combining. Retransmissions use the same MCS as the original transmission – only the transmission power is based on CQI. Thus the SIR error is ignored for retransmissions and does not contribute to the SIR error distribution.

The maximum number of retransmissions is set to 5. When the maximum is reached, the packet is retransmitted from the RLC layer. The standard as well as the simulator uses 6 parallel HARQ processes, each of them employing a stop-and-wait scheme. The number of processes has been adapted to the roundtrip time, so that the transmission shall be continuous.

4.3 Implementations

CQI adjustment

CQI adjustment has been implemented in the simulator according to [2] and the description in Section 2.6.2, and with the default parameter values presented in [15]. It can be switched on or off by changing one parameter. The BLEP_{target} for CQI adjustment can be chosen by changing parameters $nackPlus$ and $nackMinus$. The channel quality offset is optimized for low speed (explained further in Section 5.1).

Robust link adaptation

Robust link adaptation can be turned on or off. When on, the channel quality offset will depend on the UE mean speed, v_{mean}, and BLEP_{target}. With these two parameters, a 2D table lookup can be made to find a suitable offset in a given system. The channel quality offset can be MCS dependent or not, depending on whether it is needed to be.

An additional bias offset will make sure that $E[\Gamma_{t+d}] = \Gamma_t$.

Logging

The following variables are logged for the purpose of determining results:

- SIR error, Γ_e is logged for all blocks. The purpose is to determine the SIR error distribution.
- BLEP is logged for all blocks. The log can be used to determine the mean BLEP and thus the channel quality offset. It can also be used in later simulations to see what BLEP is reached using CQI adjustment or robust link adaptation.
- Number of downloaded bits and downloading time is logged per user. This information can be used to determine both user throughput and system throughput.

Chapter 5

Simulation Results

Using the theory of Chapter 2, the ideas introduced in Chapter 3 and the models and assumptions from Chapter 4, simulations have been conducted. This chapter will present the results, explain and discuss them.

5.1 Simulated Cases

This thesis aims to test whether or not the robust link adaptation algorithm results in a stable BLER, equal to BLER_{target}. The wish is to do better than existing methods. If one is able to control the BLER efficiently, one can optimize it for highest possible throughput. Two main cases will be compared in terms of BLER controllability and stability:

- *Reference case* (Ref). Employs the CQI adjustment algorithm. The channel quality offset used is optimized for $v_{mean} = 3$ km/h, and is dynamic with respect to BLER_{target}.
- *Robust case* (Rob). Employs the robust link adaptation algorithm.

There is reason to believe that CQI adjustment, which relies on HARQ statistics, will have worse performance when packets are small and less statistics are available. Two different packet sizes will be simulated in order to discover such effects:

- *Small packets.* Packet size is 10 kB, common in for example web browsing. With this size, packets are transmitted in only a couple of TTIs, and CQI long-term adjustment will rarely or never take effect. 90% of the TBSZs will fit 10 kB in 5–30 transport blocks. An offered load of 1 Mbps/cell is used, which leads to the arrival intensity $\lambda = 12.5$ users/s.
- *Large packets.* Packet size is 1000 kB, simulating large file downloads. A large number of ACKs and NACKs will be collected. An offered load of 2 Mbps/cell is used, which leads to the arrival intensity $\lambda = 0.25$ users/s.

The SIR error distribution is severely affected by the UE speed. Robust link adaptation will take that into account by having speed dependent channel quality offset. To prove the efficiency of this, four different UE speeds have been simulated:

- $v_{mean} = 3$ km/h. A typical pedestrian.
- $v_{mean} = 10$ km/h. A runner or slow vehicle.
- $v_{mean} = 50$ km/h. A typical vehicle.
- $v_{mean} = 120$ km/h. A fast vehicle or train.

Channel coherence time and correlation coefficient at the different v_{mean} are presented in Table 5.1.

Table 5.1: Channel coherence time and correlation coefficient at the simulated v_{mean}

	Channel coherence time, T_c	Correlation coefficient, ρ
$v_{mean} = 3$ km/h	180 ms	0.257
$v_{mean} = 10$ km/h	54.0 ms	0.029
$v_{mean} = 50$ km/h	10.8 ms	0.013
$v_{mean} = 120$ km/h	4.50 ms	0.010

The motivation for a controllable and stable BLER is to maximize throughput. Throughput can be approximated as $TP = R(1 - BLER)$, R being the information bit rate at the chosen TBSZ. Choosing a larger TBSZ for a specific SIR will not only increase R, but also BLER. Hence it is not obvious what BLER_{target} to aim for, that will maximize throughput. Four different BLER targets will be evaluated. The goal is to see which of them maximizes throughput, and how well the two algorithms can keep $\text{BLER} = \text{BLER}_{target}$.

- $\text{BLER}_{target} = 10\%$
- $\text{BLER}_{target} = 20\%$
- $\text{BLER}_{target} = 30\%$
- $\text{BLER}_{target} = 40\%$

For throughput simulations, the offered load is varied in steps of 200 kbps for small packet sizes, and 400 kbps for large packet sizes. It goes from $200, ..., 1000$ kB and $400, ..., 2000$ kB, respectively.

5.2 Determining SIR Error Distribution

To determine the channel quality offset, initial simulations are run with neither CQI adjustment nor robustness. Each cell contains 10 users, each downloading an infinite file. The number of observations of Γ_e is in the order of 10^6 and the resulting distributions are depicted in Figure 5.1. The difference between 50 km/h and 120 km/h is very small. This can be explained by the small difference in correlation coefficient, ρ, in Table 5.1.

The distributions closely resembles Normal distributions which can be described merely by their mean value and variance. From this, the next step of determining channel quality offset can be pursued.

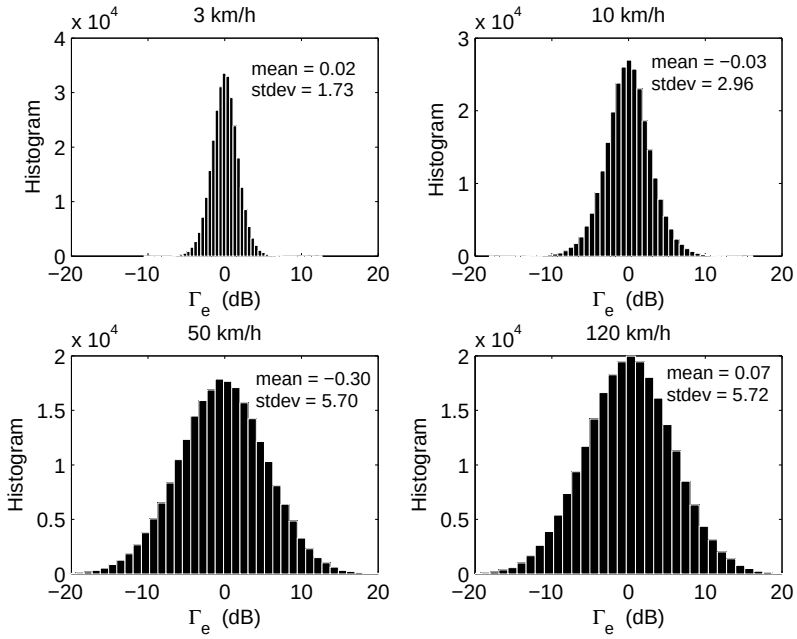

Figure 5.1: Empirical distribution of Γ_e at the different v_{mean}

5.3 Determining Channel Quality Offset

By simply varying the mean value of $\Gamma_{t+d} = \Gamma_t + \Gamma_e$, curves such as in Figure 3.6 can be generated. Recall that Γ_e is assumed unbiased, thus only Γ_t is varied. Figure 5.2 merges Figures 3.5 and 3.6, illustrating the link curves for robust link adaptation at different speeds, as well as for ordinary link adaptation.

From the figure, it is possible to determine channel quality offset for any BLER_{target}. That has been done for the BLEP targets investigated. The resulting channel quality offsets for all SIR thresholds available in the MCS table are presented in Figure 5.3.

From the offsets in the figure, bias has not yet been removed. As can be seen from the figure, the channel quality offset is fairly constant over the SIR thresholds (and thus MCS). Using the average channel quality offset over all MCSs does not hurt the performance significantly. A static offset is also easier from an implementation point of view. Table 5.3 is used to find a suitable channel quality offset at different v_{mean} and BLER_{target}. The offsets in the table include bias compensation.

5.4 Graphical Results

This section will present the graphical results from the simulations. Discussions and thoughts about the results are carried out in Section 5.5.

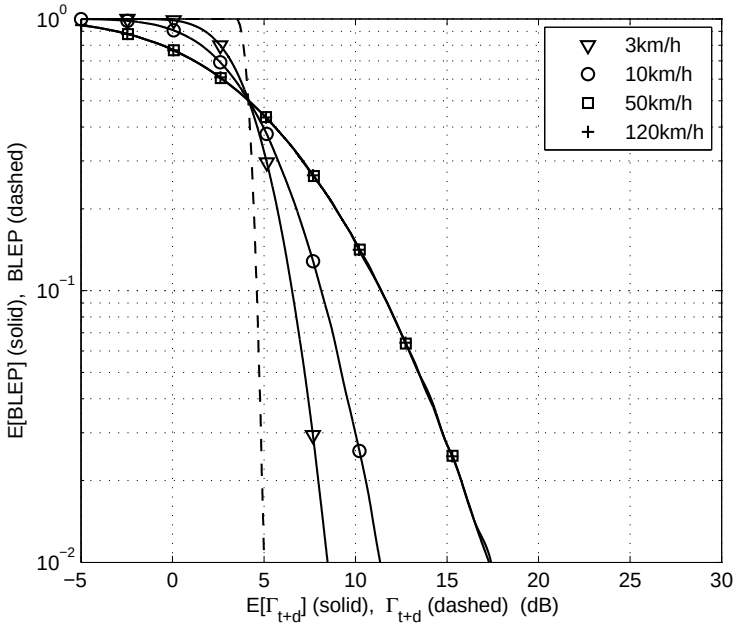

Figure 5.2: Basis for determining channel quality offset at the different v_{mean} and a certain MCS n

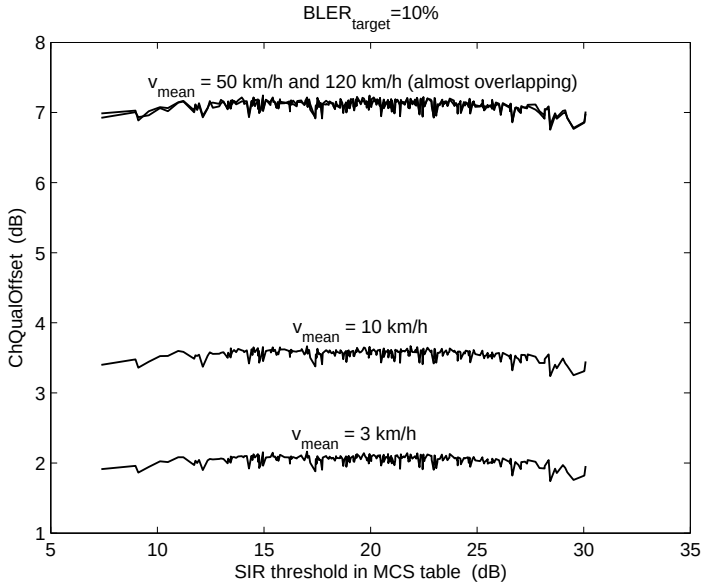

Figure 5.3: Channel quality offset versus SIR threshold at the different v_{mean}

5.4.1 BLER Stability

The intention is to show which one of the cases *Ref* and *Rob* gives the most stable and controllable BLER. In Figures 5.4-5.5 the two cases are compared in

Table 5.2: All channel quality offsets used in the simulations

v_{mean} / BLER_{target}	3 km/h	10 km/h	50 km/h	120 km/h
10%	2.0628	3.5131	6.7750	7.1483
20%	1.3668	2.3003	4.3498	4.7197
30%	0.8635	1.4255	2.5993	2.9696
40%	0.4332	0.6772	1.1044	1.4726

terms of BLER vs. speed. Two different BLER targets are presented here, the other two can be found in Appendix A. The plots show that CQI adjustment performs quite well at low speeds and large packet sizes. Robust link adaptation has the same performance for both packet sizes, and keeps the BLER close to the target even at high speeds. It can also be noted that the BLER is a bit too low at 3 km/h, in both figures. This is discussed in Section 5.5.

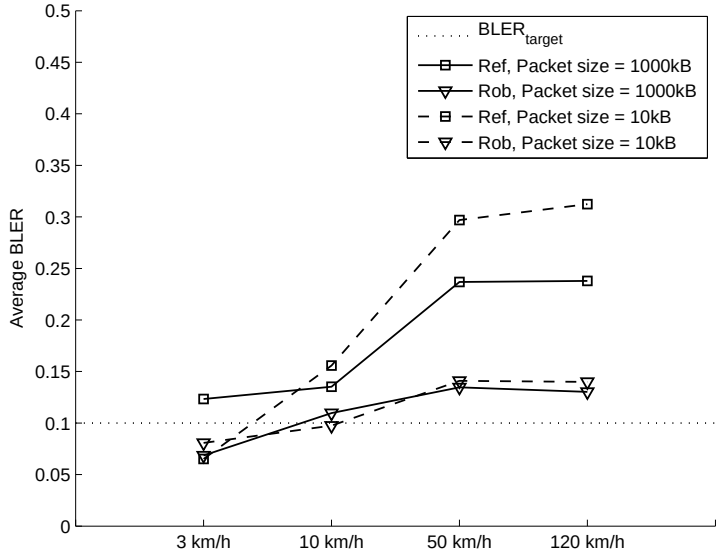

Figure 5.4: BLER stability, $\text{BLER}_{target} = 10\%$, comparing *Ref* and *Rob*

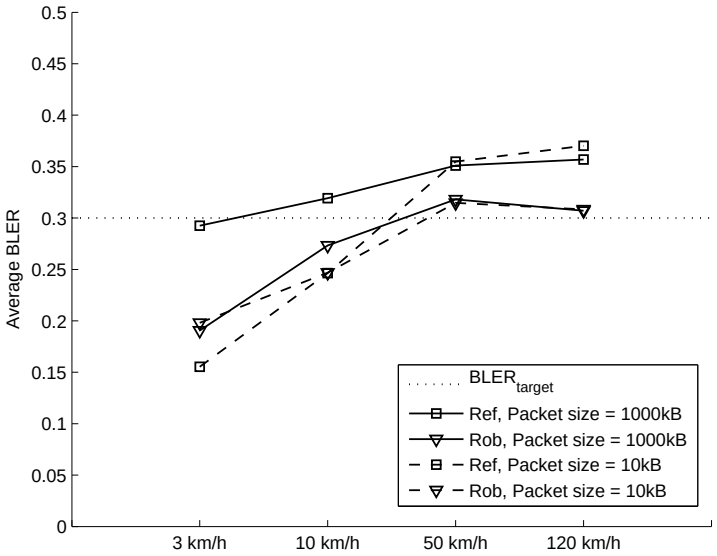

Figure 5.5: BLER stability, $\text{BLER}_{target} = 30\%$, comparing *Ref* and *Rob*

5.4.2 Throughput

Here, the intention is to show at what BLER target maximum throughput is achieved. It does not matter which link adaptation algorithm is used, only the trade-off between BLER and TBSZ matters. Average user throughput is defined as the mean number of downloaded bits per user, divided by the time they were active – including the channel setup time. Average cell throughput is defined as the total number of bits downloaded in the system, divided by the simulation time and number of cells. A low speed case and a high speed case is presented in Figures 5.6-5.7. At low speed and large packet size, CQI adjustment keeps the BLER target very well, as was seen in Figures 5.4-5.5. Therefore CQI adjustment is the algorithm used when comparing throughput at different BLER targets. At high speed on the other hand, robust link adaptation is used. The results show that it is better to aim for low BLER at low speeds, and high BLER at high speeds.

5.4.3 Special Cases

Algorithms combined

One test was carried out, letting robust link adaptation work together with CQI adjustment at high speed, where CQI adjustment has shown to perform badly. The resulting average BLER compared to *Ref* and *Rob* is presented in Table 5.3. We note that CQI adjustment makes the BLER too high, even when it has a good starting point.

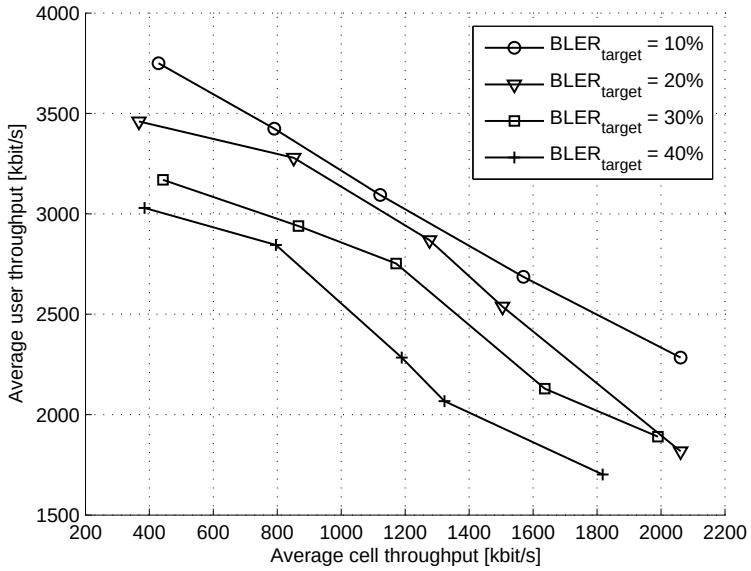

Figure 5.6: Throughput comparison at different BLER_{target} when v_{mean} = 3 km/h and $Packet\ size = 1000$ kB

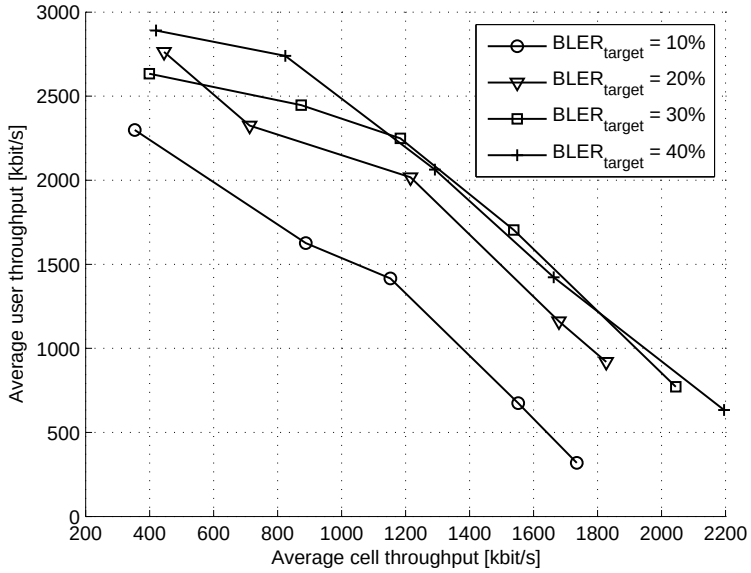

Figure 5.7: Throughput comparison at different BLER_{target} when v_{mean} = 50 km/h and $Packet\ size = 1000$ kB

Other Receiver Types

In a real system, it is very difficult to know what receiver type the UEs employ. The procedure of finding channel quality offset is the same regardless of receiver

Table 5.3: Average BLER when $\text{BLER}_{target} = 10\%$ and $v_{mean} = 50$ km/h

	10 kB	1000 kB
Ref	29.7%	23.7%
Rob	14.1%	13.5%
Both	22.1%	22.5%

type, but one has to make an assumption. In these simulations GRAKE2 receivers were used. Different receiver types can be unequally good at mitigating interference and self-interference. If GRAKE1 receivers use the same channel quality offsets as were calculated for GRAKE2, what will the performance be like? Figure 5.8 compares the average BLER for the two receiver types using the same offsets. A comparison of the Γ_e distribution is depicted in Figure 5.9.

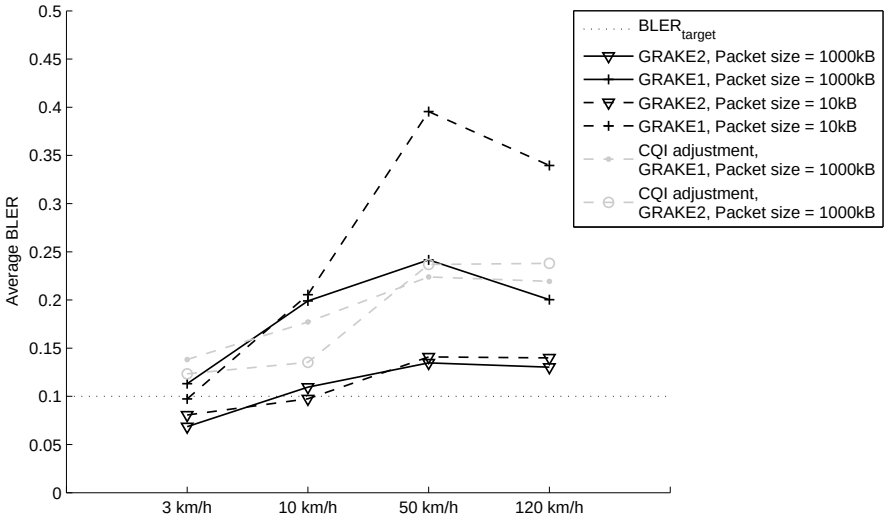

Figure 5.8: BLER stability, $\text{BLER}_{target} = 10\%$, comparing *GRAKE2* and *GRAKE1* in a robust system

Other Channel Models

In all simulations the Pedestrian A channel model was used. Another common model is the *3GPP Typical Urban* (TU). The procedure of determining offsets would be exactly the same for any channel model. It is interesting to see though, how the CQI error distribution Γ_e and hence the offsets are different in other channels. At 50 km/h, the difference can clearly be seen in Figure 5.10. The distribution for TU is about half as wide as for PedA, leading to another channel quality offset. A PedA channel has one very strong tap and thus varies a lot as this tap fades up and down. A TU channel has a large number of weak taps which makes the total fading magnitude smaller.

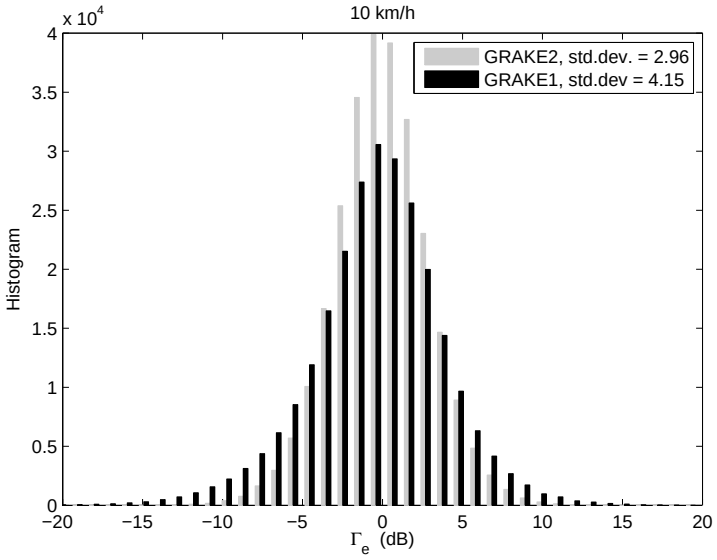

Figure 5.9: Γ_e distribution for GRAKE2 and GRAKE1 receivers, $v_{mean} = 10$ km/h

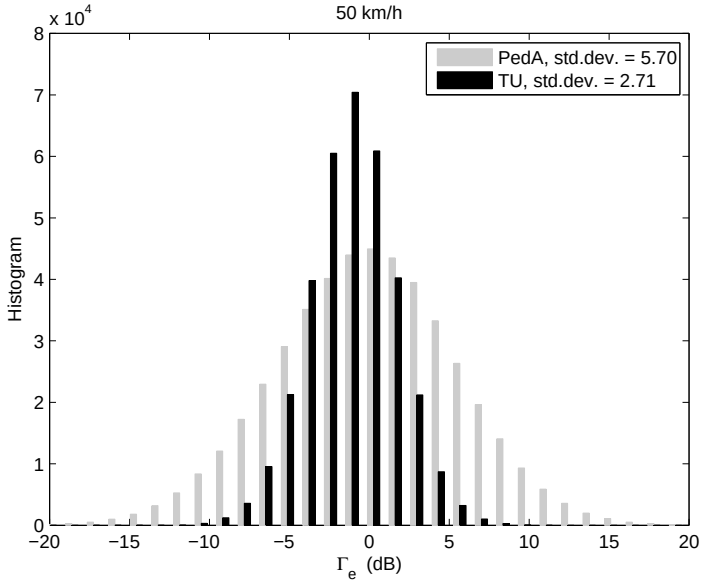

Figure 5.10: Γ_e distribution for PedA and TU channels, $v_{mean} = 50$ km/h

5.5 Discussion

CQI adjustment, small packets

As can be seen in Figures 5.4-5.5, CQI adjustment does not manage to adjust BLER correctly. It is clear that the packets are too small to have enough

time to adjust the BLER. Only the short-term adjustment is active during the time the few blocks that are being sent. The mean TBSZ that is being used is approximately 1.3 kB. That gives a number of transport blocks equal to 8. During the transmission, CQI can be adjusted downwards 4 times, but upwards none – making the algorithm more safe than accurate. At 3 km/h, the CQI is correct initially, but CQI adjustment is seen to lower it, leading to a lower BLER. At 50 and 120 km/h, CQI is initially incorrect, and CQI adjustment doesn't manage to lower it enough during the limited time it has. Because of the steep uphill, the conclusion is that CQI adjustment in this case leads to an *unstable* BLER, with respect to speed variations.

CQI adjustment, large packets

At low speeds (3 and 10 km/h), CQI adjustment performs quite well here. The first reason for this is the initial channel quality offset, which is optimized for low speeds. Secondly, it has a long time to gather statistics and adjust CQI accordingly. The mean BLER is too high at 50 and 120 km/h. With a mean TBSZ of about 1.3 kB, the long-term adjustment will be able to adjust CQI about 15 times during one packet transmission. At high speeds, CQI may have to be adjusted downwards by several dB (as seen in Figure 5.3), which takes time. This could be one reason for high BLER. It is also worth noting that investigations on CQI adjustment performance, such as in [15], shows that the algorithm is unstable and tends to result in an average BLER which is a bit too high.

The high BLER at 50 and 120 km/h may also be the result of an anti-windup that was introduced for CQI adjustment. A hardcoded limitation makes sure that $\text{abs}(\Delta CQI - \text{ChQualOffset}) \leq 4$ dB (ChQualOffset is considered a positive number in this thesis). This means that CQI adjustment may not be able to adjust the CQI downwards as much as needed at 50 or 120 km/h. To see if this effect was true, $\text{abs}(\Delta CQI - \text{ChQualOffset})$ was logged for the 50 km/h case, see Figure 5.11. Both when aiming for 10% and 30%, very few CQI reports were adjusted by more than 4 dB. Hence, this is not enough to explain the bad performance of CQI adjustment.

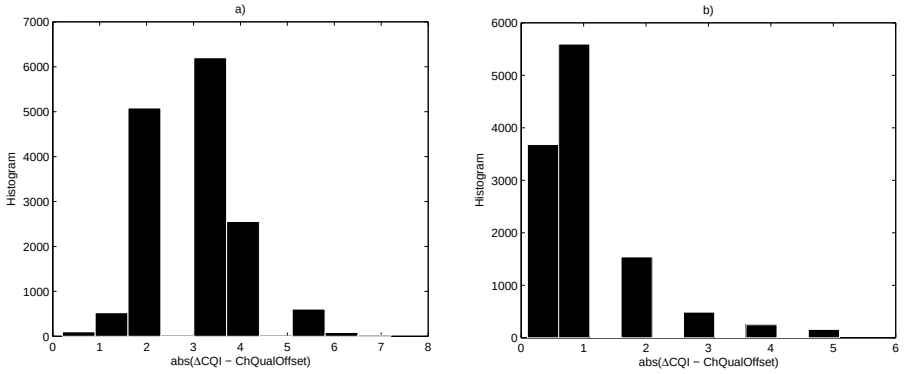

Figure 5.11: $\text{abs}(\Delta CQI - \text{ChQualOffset})$ at 50 km/h when a) $\text{BLEP}_{\text{target}} = 10\%$, and b) $\text{BLEP}_{\text{target}} = 30\%$

Robust link adaptation

Looking at the figures, one can note that there is almost no performance difference between the two packet sizes. This is expected, since robust link adaptation does not need ACK/NACK reports. One can also see that the slope of the curves is less steep than in the reference case, meaning that robust link adaptation keeps the BLER more stable when the speed is increasing. One problem that is seen, is that BLER is much too low at 3 km/h. The channel quality offsets were determined at a high load with a certain interference situation. The load is lower and the interference situation is not the same in the simulations. At 3 km/h the CQI error is barely affected by the Doppler spread, so here the interference variations are dominant. Since the interference variation may be lower (due to less interfering power) in the simulations, BLER is too low.

Special cases

- Using CQI adjustment in a robust link adaptation system clearly makes the performance worse at high speeds. It was seen in Figures 5.4-5.5 that CQI adjustment did not manage at high speed, even if the packet size is large. When using both algorithms, CQI will initially be correct *and* when the packet size is large, CQI adjustment will have time to correct any errors. Despite this, the average BLER is too high. This shows the instability of CQI adjustment.

- Using the same channel quality offsets for GRAKE2 and GRAKE1 showed not to work. For all speeds except 3 km/h, the average BLER is too high, seen in Figure 5.8. The reason is the different variance in the Γ_e distributions. Another set of offsets would have been needed in order to have the same performance with GRAKE1 receivers. This is a problem since there is no way to know what receivers are in the network. CQI adjustment shows similar performance regardless of receiver type.

- The channel type has a clear influence on the Γ_e distribution, as seen in Figure 5.10. As the number of taps and power of each tap changes, the variations in fast fading change in severity. Channel quality offsets have to be determined for each channel type, but luckily it is possible to estimate the channel if one assumes reciprocity between uplink and downlink.

Throughput, low speed

From Figure 5.6 it is clear that the highest throughput is achieved when $\text{BLER}_{target} = 10\%$. The throughput is then decreasing when BLER_{target} increases. The difference in throughput between $\text{BLER}_{target} = 10\%$ and $\text{BLER}_{target} = 40\%$ is 20-25%.

Throughput, high speed

At 50 km/h, the situation is the opposite to 3 km/h. $\text{BLER}_{target} = 10\%$ gives the lowest throughput. At low loads, $\text{BLER}_{target} = 40\%$ maximizes throughput, while at higher loads there is no significant difference between $\text{BLER}_{target} = 40\%$ and $\text{BLER}_{target} = 30\%$.

The optimum BLER_{target} is dependent on speed. This is most easily explained by an example. Start from Figure 5.2 or Table 5.2. At 3 km/h there is only a small difference in channel quality offset between aiming at 10% or at 40%. Therefore the TBSZ (and thus rate R) will not differ much. For the same rate, it is obviously better to have as low BLER as possible in order to maximize throughput. At 50 km/h, aiming for 40% BLER results in a much larger TBSZ, which to some extent compensates for the high BLER – and high throughput is achieved.

Chapter 6

Conclusions

Accurate link adaptation is essential in today's mobile systems where data rates are increasing and the error tolerance is decreasing. This master thesis project has aimed to take the CQI inaccuracy into account and to implement and evaluate a robust link adaptation. The goal of the new algorithm has been to obtain stability and controllability of the average BLER. Once that has been achieved, the BLER can be controlled to maximize throughput. The report focuses on the downlink, i.e. HSDPA.

In today's systems, Modulation and Coding Scheme (MCS) is chosen based on the instantaneous estimated SIR, trying to achieve BLEP = BLEP_{target}. The estimated SIR though, is stochastic with a distribution depending on measurement error, quantization error and delay. As a result, the average BLER will be too high. The higher the UE speed is, the more the delay matters to the SIR distribution. In a robust link adaptation system, MCS is chosen based on the average estimated SIR that results in $E\left[\text{BLEP}\right] = \text{BLEP}_{target}$.

A reference system using CQI adjustment was compared to a robust link adaptation system in terms of BLER stability and controllability. Robust link adaptation shows a clear stability in keeping the average BLER close to the BLER target at different UE speeds. The stability is achieved by having speed dependent channel quality offsets. Robust link adaptation aims for a target BLER by having BLEP_{target} dependent channel quality offsets. The algorithm shows most gain at high speeds, from 50 km/h and up. For small packet transmissions, it is better than CQI adjustment at all speeds. For large packet transmissions, it is better above 50 km/h.

One disadvantage of robust link adaptation is that it needs to assume or estimate UE speed, UE measurement error, channel type, receiver type and interference levels. There are ways to assess all of these factors, but not receiver type. Since there might be different receiver types in the network, no BLER can be guaranteed. If CQI adjustment can be made stable at high speeds, it can be used in conjunction with robust link adaptation to compensate for such errors.

CQI adjustment is optimal when the speed is low (3 or 10 km/h) and packet

size is large. At higher speeds it gets too unstable to manage the adjustment. For small packets it usually only has time to adjust CQI downwards, so a good initial CQI is essential for it to be reasonably accurate. Using robust link adaptation to initially adjust CQI can only make CQI adjustment better. A system with both robust link adaptation and CQI adjustment will be robust to some extent, but also be able to manage with eventualities such as different receivers and UE measurement bias.

The user throughput depends on the target BLER, and the target BLER which maximizes throughput depends on the UE speed. At 3 km/h, throughput increases when target BLER *decreases* (only 10%, 20%, 30% and 40% were tried). At 50 km/h, throughput increases when target BLER *increases*. The exact dependency of throughput as a function of target BLER and speed has not been derived in this work. This is subject for future work. By taking advantage of the BLER controllability and stability with robust link adaptation, optimum target BLER can be chosen.

6.1 Future Work

The following list presents some study items which are suitable for future work:

- How shall suitable channel quality offsets be chosen in real base stations? They can either be computed per user such that each user reaches $BLER_{target}$ on average, or for all users such that the system reaches $BLER_{target}$ on average. Either way, the users speed has to be assessed in some way. Shall this be done by means of speed estimation in the NodeB, and in that case, how accurate can the estimation be made?

- An extensive investigation on how to optimize throughput. This work has shown that throughput is a function of $BLER_{target}$ and v_{mean}. Can $BLER_{target}$ be made dynamic at varying UE speed? Again, this supposes that v_{mean} is assessed in some way. The throughput should also be evaluated at higher layers where it might be affected by delays caused be frequent retransmissions.

- CQI adjustment has shown to be unstable at high speeds – when used in conjunction with robust link adaptation it destroys some of the good performance. Can CQI adjustment be optimized to work well at high speeds? Even if robust link adaptation has shown good performance, CQI adjustment must remain to cope with unexpected CQI bias and different receivers.

- Look at UEs supporting 64QAM and MIMO. These have another mapping to CQI when the SIR is above a certain knee. Also, each MIMO stream uses only a 4-bit CQI report.

- Robust link adaptation is subject to use in any communication system with link adaptation. The algorithm should be investigated in and adapted to LTE.

References

[1] E. Dahlman, S. Parkvall, P. Beming and J. Sköld, "3G Evolution: HSPA and LTE for Mobile Broadband", Elsevier Ltd., 2007

[2] Seungtai Kim, Anders Jonsson, Anders Milén, Fredrik Ovesjö and Samuel Axelsson, "HS-DSCH scheduler and downlink layer 2 and layer 1 functions and algorithms", 402/155 17-HSD 101 02/6 Uen, 2008

[3] D. Martín-Sacristán, J. F. Monserrat, D. Calabuig and N. Cardona, "HSDPA Link Adaptation Improvement Based on Node-B CQI Processing", ISWCS, Wireless Communication Systems, 2007

[4] H. Touheed, A. Ul Quddus, R. Tafazolli, "An Improved Link Adaptation Scheme for High Speed Downlink Packet Access", Vehicular Technology Conference, 2008

[5] O. Enander, "UE Feedback Optimisation in HSDPA", Ericsson AB, FJW/SR, 2008

[6] S. Y. Jeon, D. H. Cho, "An Enhanced Channel-Quality Indication (CQI) Reporting Scheme for HSDPA Systems", IEEE COMMUNICATIONS LETTERS, VOL. 9, NO. 5, MAY 2005

[7] 3GPP TS 25.401 V7.6.0, "Technical Specification Group Radio Access Network; UTRAN overall description (Release 7)" 2008

[8] 3GPP TS 25.308 V7.8.0, "High Speed Downlink Packet Access (HSDPA), Overall description", Stage 2, 2008

[9] 3GPP TS 25.214 V7.9.0, "Technical Specification Group Radio Access Network, Physical layer procedures (FDD)", 2008

[10] M. Nakagami, "The m-Distribution: A General Formula of Intensity Distribution of Rapid Fading" in Statistical Methods in Radio Wave Propagation, Pergamon Press: Oxford, U.K., 1960

[11] A. J. Goldsmith, M-S. Alouini, "Adaptive Modulation over Nakagami Fading Channels" Wireless Personal Communications, vol. 13, pp. 119-143, Kluwer Academic Publishers: Netherlands, 2000

[12] A. Simonsson, "CQI, BLER & TBS Measurement Analysis", EAB-05:010777 Uen, 2005

[13] 3GPP TS 25.814 V7.1.0, "Technical Specification Group Radio Access Network, Physical layer aspects for evolved Universal Terrestrial Radio Access (UTRA)", 2006

[14] 3GPP TS 25.306 V7.8.0, "Technical Specification Group Radio Access Network, UE Radio Access capabilities", 2008

[15] N. Wiberg, "Performance of some CQI Adjustment Algorithms" EAB/TB-04:000329 Uen, 2004

Appendix A

Additional BLER Plots

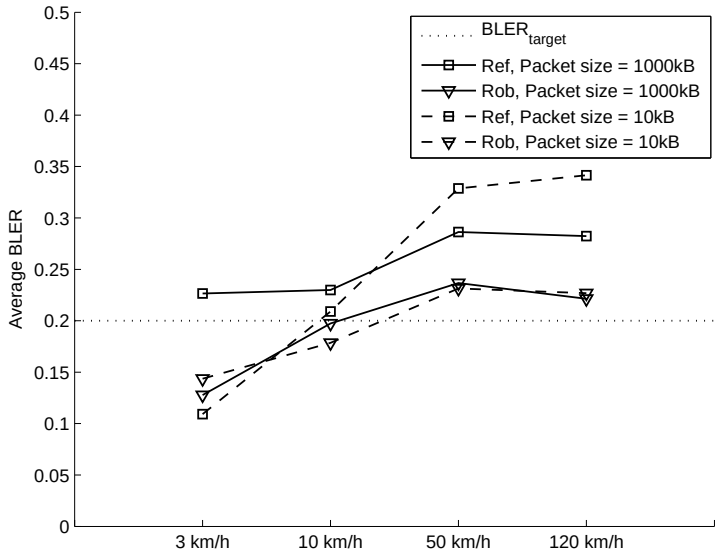

Figure A.1: BLER stability, $\text{BLER}_{target} = 20\%$, comparing *Ref* and *Rob*

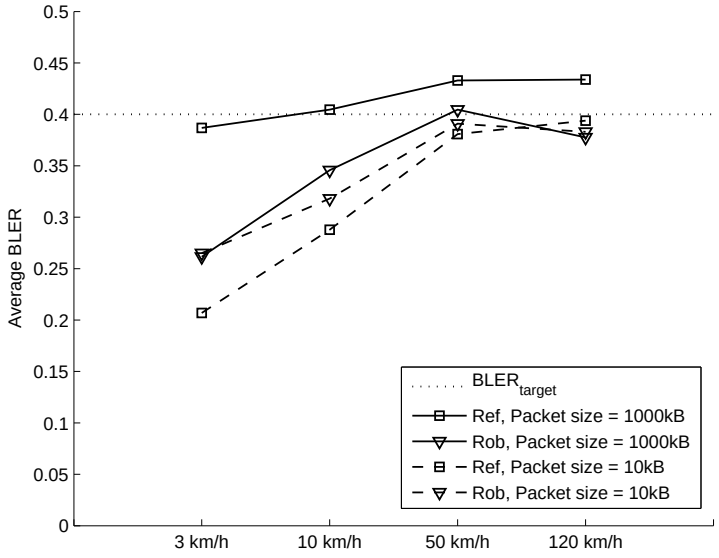

Figure A.2: BLER stability, $\text{BLER}_{target} = 40\%$, comparing *Ref* and *Rob*

Appendix B

Simulation Parameters

Table B.1: System Parameters

Number of sites	3
Sectors per site	3
Site-to-site distance	1500 m
Antenna dimension	2D
Antenna height	30 m

Table B.2: Channel Parameters

Okumura-Hata parameter C	-29.0125
Okumura-Hata parameter β	-3.5225
Shadow fading standard deviation	8 dB
Decorrelation distance	100 m
Fast fading map	PedA
Receiver type	GRAKE2

Table B.3: Traffic Parameters

User arrival process	Poisson(λ)
User placement	Uniform
UE category	8
TCP model	Disabled

Table B.4: Radio Resource Management Parameters

Scheduler	Round Robin
SIR measurement error	N(0,1) dB
HS measurement power offset, ϕ	7 dB
Quantization error	U(-0.5, 0.5) dB
CQI reporting delay, d	4 ms
CQI reporting interval	8 ms
CQI adjustment averaging length, M	50
$nackPlus$	$\text{BLEP}_{target} - 0.02$
$nackMinus$	$\text{BLEP}_{target} + 0.02$
Switchpoint, short-term→long-term, $ackNackSum$	15
Number of parallel HARQ processes	6
Max number of retransmissions	5